Off-axis electric field of a ring of charge

Fredy R. Zypman[a]

Department of Physics, Yeshiva University, New York, New York 10033-3201

We consider the electric field produced by a charged ring and develop analytical expressions for the electric field based on intuition developed from numerical experiments. Our solution involves the approximation of elliptic integrals. Problems are suggested for an arbitrarily charged ring. © *2006 American Association of Physics Teachers.*
[DOI: 10.1119/1.2149869]

I. INTRODUCTION

The use of numerical methods in physics courses is already a mature practice. This use is true in particular in electricity and magnetism, where standard textbooks have incorporated new chapters,[1] sections,[2–4] examples,[5] and problems.[6] Many articles have introduced instructional material using numerical methods.[7–16]

We consider the problem of finding the electrostatic potential in all space produced by a charged ring. In most analytical approaches to this problem, the solution is found only along the symmetry axis of the ring, where the integrals can be expressed in terms of elementary functions. The off-axis problem is avoided because it involves special functions that are unfamiliar to most undergraduates. We surmount this difficulty by plotting the relevant numerical integrals and through trial and error develop intuition about the expected form of the solution. The expected form is used to construct a hypothesis about the form of the solution. We test this hypothesis and propose simple, useful formulas for the electrostatic field.

II. FIELD PRODUCED BY A UNIFORMLY CHARGED RING

Figure 1 shows the system of interest. A charged ring of radius a rests in the xy plane with its center at point $\mathbf{0}$. A generic source point $\mathbf{r}'$ is parametrized by the angle α that it makes with $\hat{i}$, a unit vector:

$$\mathbf{r}' = a \cos \alpha \hat{i} + a \sin \alpha \hat{j}. \tag{1}$$

The observation point $\mathbf{r} = (x, y, z)$ is located anywhere in space. Due to axial symmetry, we do not lose generality by calculating the field at $\mathbf{r} = (x, 0, z)$. We write the distance to the origin as $r = a\xi$ and let θ be the angle between $\mathbf{r}$ and $\hat{k}$:

$$\mathbf{r} = a\xi \sin \theta \hat{i} + a\xi \cos \theta \hat{k}. \tag{2}$$

We let Q be the total charge in the ring and write the electric field as

$$E = \frac{1}{4\pi\varepsilon_0} \frac{Q}{2\pi a} \int_{Ring} \frac{\mathbf{r} - \mathbf{r}'}{|\mathbf{r} - \mathbf{r}'|^3} d\mathbf{r}' \tag{3a}$$

$$= \frac{1}{4\pi\varepsilon_0} \frac{Q}{2\pi a} \frac{1}{a} \int_0^{2\pi} \frac{(\xi \sin \theta - \cos \alpha)\hat{i} - \sin \alpha \hat{j} + \xi \cos \theta \hat{k}}{(1 + \xi^2 - 2\xi \sin \theta \cos \alpha)^{3/2}} d\alpha. \tag{3b}$$

The integral in the $\hat{j}$ direction vanishes as expected because a test charge at $\mathbf{r}$ does not sense a torque along the symmetry axis. The other integrals are functions of α only through $\cos \alpha$. Because $\cos \alpha$ is an even function with respect to $\alpha = \pi$, we can make the substitution $\int_0^{2\pi} \rightarrow 2\int_0^{\pi}$. The components of the electric field are

$$E_x = \frac{1}{4\pi\varepsilon_0} \frac{Q}{\pi a^2} \left\{ \frac{\xi \sin \theta}{(1 + \xi^2)^{3/2}} f_1(\mu) - \frac{1}{(1 + \xi^2)^{3/2}} f_2(\mu) \right\}, \tag{4a}$$

$$E_z = \frac{1}{4\pi\varepsilon_0} \frac{Q}{\pi a^2} \left\{ \frac{\xi \cos \theta}{(1 + \xi^2)^{3/2}} f_1(\mu) \right\}, \tag{4b}$$

where we have introduced

$$\mu = \frac{2\xi}{1 + \xi^2} \sin \theta, \tag{5}$$

$$f_1(\mu) = \int_0^{\pi} \frac{d\alpha}{(1 - \mu \cos \alpha)^{3/2}}, \tag{6}$$

$$f_2(\mu) = \int_0^{\pi} \frac{\cos \alpha \, d\alpha}{(1 - \mu \cos \alpha)^{3/2}}. \tag{7}$$

At this stage, the expressions have been reduced as much as possible. Further advance requires evaluating the elliptical integrals in Eqs. (6) and (7). Students' unfamiliarity with these functions justifies a numerical approach. The goal of this approach is not to achieve high accuracy, but to obtain an approximation that will bring insight into the behavior of the electric field.

The first step is to plot $f_1(\mu)$ and $f_2(\mu)$. To this end, we use MATHEMATICA because our school has a site license. Figure 2 shows the first three statements of the program. The function $f_1(\mu)$ is plotted by creating a list of pairs $\{\mu, f_1(\mu)\}$. Note that the physical restrictions $0 \leq \theta \leq \pi$ and $\xi > 0$ bound μ to the interval $[0, 1]$. From the plot in Fig. 3 we see that the function looks smooth for $\mu < 1$ and appears to diverge at $\mu = 1$. This behavior is reasonable because we expect the
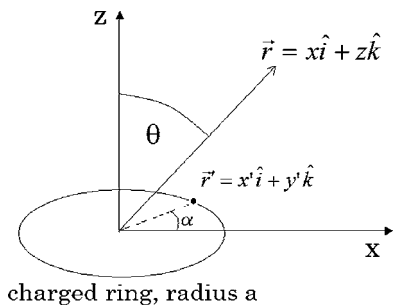
Fig. 1. The charged ring produces an electric field at the point **r**.

magnitude of the field to be finite at all points in space with the exception of points on the ring that are at $\xi=1$ and $\theta=\pi/2$, corresponding to $\mu=1$.

We next study numerically the nature of the divergence. Given that the field of a line charge diverges as the inverse distance and as the inverse distance squared for a point charge, we guess the divergence to be a power law. Thus, we numerically construct the quantity $(1-\mu)^\sigma f_1(\mu)$ for various σ. Figure 3 shows plots for $\sigma=0.9$, 1.1, and 1.0. We see that for $\sigma=0.9$, the divergence is still present. For $\sigma=1.1$, $(1-\mu)^\sigma f_1(\mu)$ goes to zero, indicating that σ is smaller than 1.1. On the other hand, for $\sigma=1.0$, $(1-\mu)^\sigma f_1(\mu)$ remains finite for all values of μ. Therefore, this evidence suggests that $f_1(\mu)$ diverges as $1/(1-\mu)$.

We now turn to the integral itself. Although we cannot write the integral $f_1(\mu)$ in terms of elementary functions in general, we can do so for $\mu\approx1$. We notice that when $\mu\approx1$, most of the contribution to the integral comes from the neighborhood of $\alpha=0$. Figure 4 shows the code in which we define the integrand $g_\mu(\alpha)$. We plot $g_\mu(\alpha)$ vs α in the interval $[0,\pi/4]$ for $0.95\leq\mu\leq0.99$. We see that as $\mu\to1$, the integral is dominated by values of α in $[0,0.3$ rad$]$. This domi-

```
In[1]:= f1 = ∫₀^π  1/(1 - μ Cos[α])^(3/2) dα;

In[2]:= L1 = Table[{μ, f1}, {μ, 0, 0.99, 0.01}];

In[3]:= ListPlot[L1, PlotRange → {0, 75}]
```
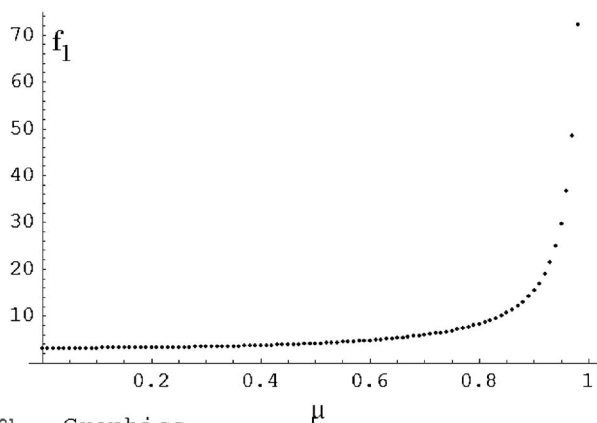


```
Out[3]= - Graphics -
```

Fig. 2. The definition, evaluation, and plot of $f_1(\mu)$.

nance suggests using $1-\alpha^2/2$ instead of $\cos\alpha$, which is accurate within 0.12% in the interval $[0,0.4$ rad$]$. Thus we consider,

$$\lim_{\mu\to1} f_1(\mu) = \int_0^\pi \frac{d\alpha}{\left[1-\mu\left(1-\dfrac{\alpha^2}{2}\right)\right]^{3/2}}, \tag{8}$$

which equals

$$\frac{\sqrt{2}\,\pi}{(1-\mu)\sqrt{2+(\pi^2-2)\mu}}.$$

Because this expression holds only for $\mu\to1$, we have

$$\lim_{\mu\to1} f_1(\mu) = \frac{\sqrt{2}}{1-\mu}, \tag{9}$$

thus confirming our hypothesis. Note that the coefficient $\sqrt{2}$ is in agreement with the graphical behavior of $(1-\mu)f_1(\mu)\approx1.4$ in Fig. 3 for $\mu\approx1$.

The $1/(1-\mu)$ dependence in Eq. (9) is due to the fact that close to the ring, the electric field of the ring is indistinguishable from that of a line of charge. For a line of charge, it is well known that the field behaves as $a/(a-r)=1/(1-\xi)\approx1/(1-\mu)$ when $r\approx a$ and $\theta\approx\pi/2$, thus justifying the divergent behavior here.

We now obtain the behavior of $f_2(\mu)$. For $\mu\approx1$, $f_2(\mu)$ should also diverge as $\sqrt{2}/(1-\mu)$ because the factor $-\alpha^2/2$ for the expansion of $\cos\alpha$ in the numerator does not contribute appreciably to the integral for $\alpha\approx0$. We check this statement numerically by plotting $[(1-\mu)/\sqrt{2}]f_2(\mu)$ in Fig. 5, where we see that this combination remains finite for all values of μ.

In our search for simple expressions we refer to Figs. 3 and 5 where we notice that the functions $[(1-\mu)/\sqrt{2}]f_1(\mu)$ and $[(1-\mu)/\sqrt{2}]f_2(\mu)$ behave linearly with μ. On this basis, we fit them to linear functions. If high accuracy were required, we could use more general polynomials, but that is not our purpose here. We perform the approximations by considering the values of the functions at the end points, namely,

$$f_1(0) = \pi, \quad \frac{1-\mu}{\sqrt{2}}f_1(\mu) \to 1 \quad \text{for } \mu\to1,$$

$$\tag{10}$$

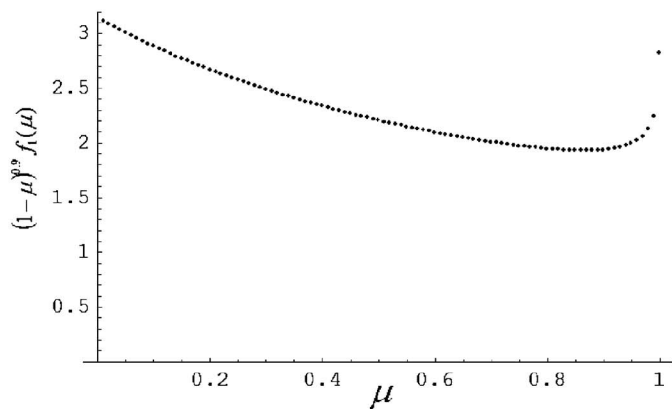$$f_2(0) = 0, \quad \frac{1-\mu}{\sqrt{2}}f_2(\mu) \to 1 \quad \text{for } \mu\to1.$$

Thus,

$$(1-\mu)f_1(\mu) \approx \pi - (\pi-\sqrt{2})\mu, \tag{11a}$$
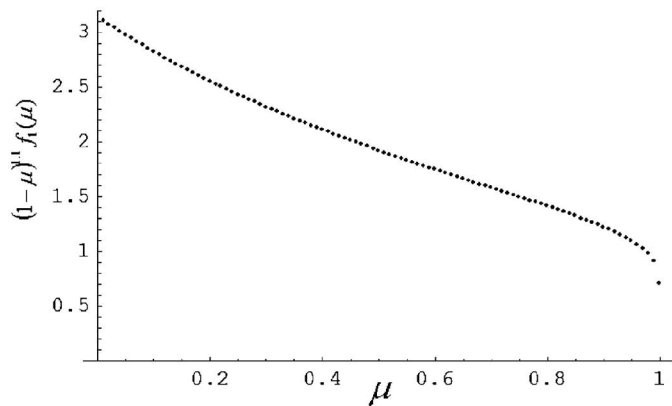
$$(1-\mu)f_2(\mu) \approx \sqrt{2}\mu. \tag{11b}$$

If we use Eq. (11) in Eqs. (4)–(7), we arrive at explicit expressions for the electric field,

In[4]:= **ListPlot[Table[{L1[[n]][[1]], L1[[n]][[2]] (1 - L1[[n]][[1]])$^{0.9}$},**
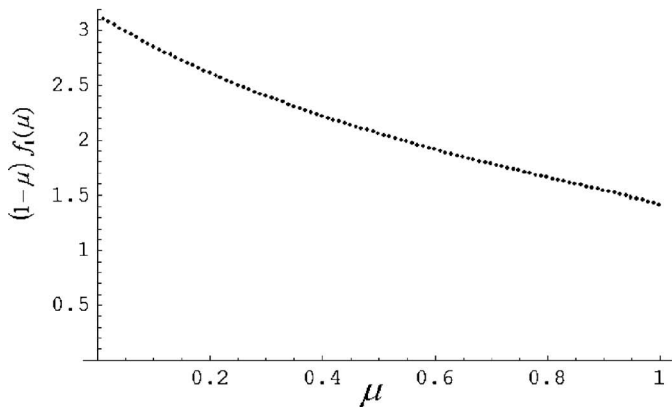   **{n, 1, Length[L1]}], PlotRange → {0, 3.2}]**

Out[4]= - Graphics -

In[5]:= **ListPlot[Table[{L1[[n]][[1]], L1[[n]][[2]] (1 - L1[[n]][[1]])$^{1.1}$},**
        {n, 1, Length[L1]}], PlotRange → {0, 3.2}]

Out[5]= - Graphics -

In[6]:= **ListPlot[Table[{L1[[n]][[1]], L1[[n]][[2]] (1 - L1[[n]][[1]])^{1}},**
        {n, 1, Length[L1]}], PlotRange → {0, 3.2}]

Out[6]= - Graphics -

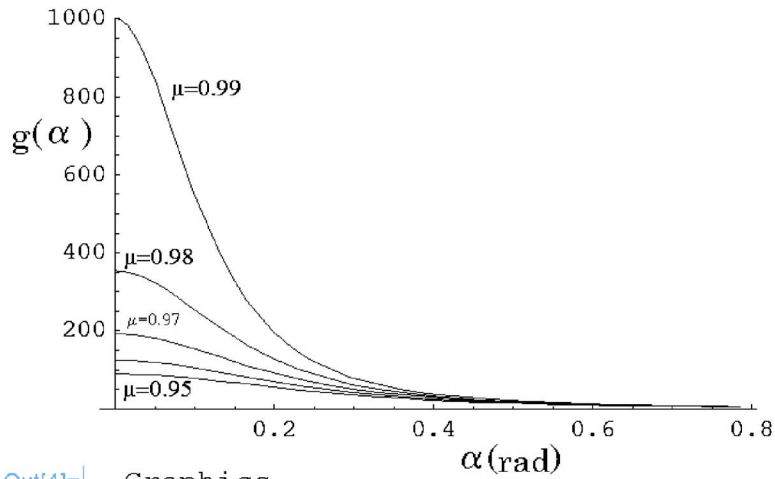Fig. 3. Plots of $(1-\mu)^\sigma f_1(\mu)$ for various values of σ.

```
In[1]:= g = 1/((1 - μ Cos[α])^(3/2));
```

```
In[2]:= m = 0;
       Do[m = m + 1;

          p[m] = Plot[g, {α, 0, π/4}, PlotRange → {0, 1000}],

          {μ, 0.95, 0.99, 0.01}];
```

```
In[4]:= Show[p[1], p[2], p[3], p[4], p[5]]
```



```
Out[4]= - Graphics -
```
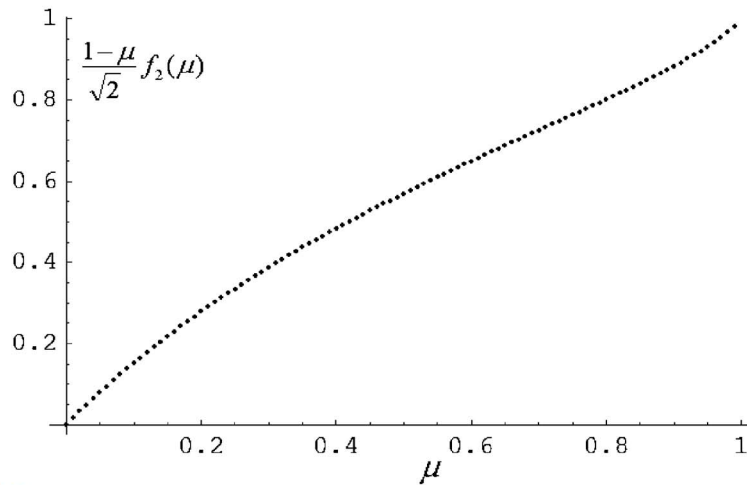
Fig. 4. Integrand of the function of interest for μ close to 1.

```
In[1]:= ListPlot[Table[{μ, (∫₀^π (Cos[α])/((1 - μ Cos[α])^(3/2)) dα) (1-μ)/√2},

          {μ, 0, 0.99, 0.01}], PlotRange → All]
```



```
Out[1]= - Graphics -
```

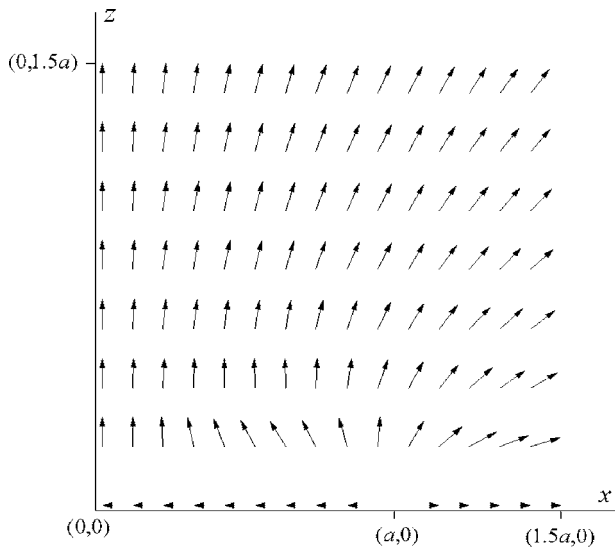Fig. 5. Plot of $[(1-\mu)/\sqrt{2}]f_2(\mu)$. The plot shows that the function remains finite for all values of μ.

Fig. 6. Electric field in the xz plane.

$$E_x = \frac{1}{4\pi\varepsilon_0}\frac{Q}{\pi a^2}\left\{\frac{\xi\sin\theta}{(1+\xi^2)^{3/2}}\frac{\pi - \dfrac{2(\pi-\sqrt{2})\xi}{1+\xi^2}\sin\theta}{1-\dfrac{2\xi}{1+\xi^2}\sin\theta}\right.$$

$$\left. -\frac{1}{(1+\xi^2)^{3/2}}\frac{\dfrac{2\sqrt{2}\xi}{1+\xi^2}\sin\theta}{1-\dfrac{2\xi}{1+\xi^2}\sin\theta}\right\}, \tag{12a}$$

$$E_z = \frac{1}{4\pi\varepsilon_0}\frac{Q}{\pi a^2}\left\{\frac{\xi\cos\theta}{(1+\xi^2)^{3/2}}\frac{\pi - \dfrac{2(\pi-\sqrt{2})\xi}{1+\xi^2}\sin\theta}{1-\dfrac{2\xi}{1+\xi^2}\sin\theta}\right\}. \tag{12b}$$

We check Eq. (12) in the limiting cases $\xi=0$ and $\xi\to\infty$. In the first case we should recover the solution for the electric field along the symmetry axis. In the second case we should obtain the Coulomb field as the leading term. We set $\xi=0$ and $\theta=0$ in Eq. (12) and correctly obtain,[17]

$$E_x = 0, \tag{13a}$$

$$E_z = \frac{1}{4\pi\varepsilon_0}\frac{Q}{\pi a^2}\left\{\frac{\xi}{(1+\xi^2)^{3/2}}\pi\right\} = \frac{Q}{4\pi\varepsilon_0}\frac{r}{(a^2+r^2)^{3/2}}. \tag{13b}$$

We next let $\xi\to\infty$ in Eq. (12) and obtain

$$E_x \to \frac{1}{4\pi\varepsilon_0}\frac{Q}{r^2}\sin(\theta), \tag{14a}$$

$$E_z \to \frac{1}{4\pi\varepsilon_0}\frac{Q}{r^2}\cos(\theta), \tag{14b}$$

which are the projections along the axes of the Coulomb field.

In Fig. 6 we show a plot of the electric field given by Eq. (12). The magnitude of an arrow has been set to a constant value to emphasize the local direction of the field. On a linear scale most arrows would be too small to be displayed due to the large values of the field near the ring at the point $(a,0)$. Figure 6 clearly shows the divergence at the ring, and the axial direction close to the axis of symmetry.

What is the importance of having off-axis information? The electric field lines give the trajectories of charged particles in that region. This information has been used extensively in the design of devices to confine charged particles (plasmas) in small volumes[18] and in the discrimination of particles according to mass (mass spectrometers).[19] Electrostatic problems with axial symmetry can be handled by summation of charged rings. Relevant problems are related to the calculations of tip-sample forces in atomic force microscopy.[20,21] Particle guns, electrostatic velocity selectors, and electrostatic ion thruster are described in Ref. 22. Electrostatic lenses are discussed in Ref. 23.

III. GENERALIZATIONS

We next consider a ring with a nonuniform charge density. This problem can be effectively used as a homework project.

The first difficulty is that, in general, the electric field does not have cylindrical symmetry. In this case, we need to work with expressions as in Eq. (3) with a linear charge density function, $\rho(\alpha)$. Although not all planes through z are equivalent, we will analyze the problem in the xz plane. There is no loss of generality because the analysis for any plane through z is the same if the origin of α is properly chosen.

Consider $\rho(\alpha)$ defined in $-\pi \leq \alpha < \pi$ and expand it around $\alpha=0$. As discussed in Sec. II, when $\mu\approx 1$ we can assume $\rho(\alpha)\approx\rho(0)$ for $\alpha\approx 0$. Therefore, we expect the divergences to behave like $1/(1-\mu)$ in this case. We then proceed as before, multiply the original integrals by $1-\mu$, and then fit these finite functions to simple polynomials.

Information about the field from a nonuniformly charged ring has a variety of applications. The quadrupolar charge distribution on a ring has been used in high precision measurements of properties of elementary particles.[24] Gravitational fields, which also satisfy Poisson's equation,[25] are useful for gravitational propulsion. A knowledge of the gravitational field produced by the rings of Saturn requires the solution of the electrostatic ring with nonuniform charge. Another example is precision measurements of the Aharonov-Bohm effect. And to study the interplay between the magnetic, electrostatic, and Aharonov-Bohm effects, a nano-ring with nonuniform potential was constructed.[26]

IV. DISCUSSION

We solved the electrostatic problem of a charged ring by finding simple solutions that retain the character of the field's behavior. Similar integrals appear for the magnetic field produced by a current ring. This problem is of particular interest because it forms the basis for understanding the parameters of Helmholtz coils. For the same reason as in the electrostatic case, the off-axis solution is usually avoided. With the expression provided in this paper, further questions can be asked regarding the homogeneity and strength of the magnetic field from the symmetry axis.

The approach used to investigate the nature of the divergence in this paper could be used in a large variety of problems, even those that have nonpower law divergences. The

idea is to build student intuition about the nature of the divergence (if it exists) via numerical exploration, which may include plotting the functions with nonlinear axes.

ACKNOWLEDGMENT

[a] Electronic mail: zypman@yu.edu

[1] R. H. Good, *Classical Electromagnetism* (Saunders, Orlando, 1999), pp. 522–533.

[2] D. L. Hatten, P. Lorrain, D. R. Corson, and F. Lorrain, *Electromagnetic Phenomena* (Freeman, New York, 2000), Sec. 9.3, pp. 174–179.

[3] I. S. Grant and W. R. Phillips, *Electromagnetism* (Wiley, Chichester, 1990), 2nd ed., Sec. 3.5.

[4] J. D. Jackson, *Classical Electrodynamics* (Wiley, Hoboken, 1999), 3rd ed., Sec. 2.12.

[5] S. V. Marshall and G. G. Skitek, *Electromagnetic Concepts and Applications* (Prentice Hall, Englewood Cliffs, NJ, 1987), 2nd ed., pp. 188–191.

[6] J. R. Reitz, F. J. Milford, and R. W. Christy, *Foundations of Electromagnetic Theory* (Addison-Wesley Longman, Reading, MA, 1993), 4th ed., p. 96, Problems 24, 25, 26.

[7] M. E. Peskin, "Numerical problem solving for undergraduate core courses," J. Comput. Methods Sci. Eng. **5**, 92–96 (2003).

[8] A. Singh, Y. N. Mohapatra, and S. Kumar, "Electromagnetic induction and damping: Quantitative experiments using a PC interface," Am. J. Phys. **70**, 424–427 (2002).

[9] G. C. McGuire, "Using computer algebra to investigate the motion of an electric charge in magnetic and electric dipole fields," Am. J. Phys. **71**, 809–812 (2003).

[10] C. Geronimi, F. Bouchut, M. R. Feix, H. Ghalila, M. Valentini, and J. M. Buzzi, "Transient electromagnetic field," Eur. J. Phys. **18**, 102–107 (1997).

[11] N. Sarlis, G. Kalkanis, C. A. Londos, S. S. Sklavounos, and P. Tsakonas, "A calculation of the surface charges and the electric field outside steady current carrying conductors," Eur. J. Phys. **17**, 37–42 (1996).

[12] S. Trester, "Computer-simulated Fresnel holography," Eur. J. Phys. **21**, 317–331 (2000).

[13] P. W. Lamberti and D. P. Prato, "A simple numerical method for solving problems in electrostatics," Am. J. Phys. **59**, 68–70 (1991).

[14] P. W. Gash, "Improved numerical solutions of Laplace's equation," Am. J. Phys. **59**, 509–515 (1991).

[15] F. Stremler, S. Klein, F. Luo, and Y. Liao, "Numerical solutions and mapping of electrostatic fields using the Apple Macintosh computer," IEEE Trans. Educ. **33**, 104–110 (1990).

[16] T. Y. Li, "Simulation of transmission lines using Mathematica," in Proceedings of the Workshop on Computational Physics, edited by M. Shapiro and J. Feagin, 18–22 June 1990, Fullerton State University, pp. 85–100.

[17] G. L. Pollack and D. R. Stump, *Electromagnetism* (Addison-Wesley, San Francisco, 2002), pp. 51, 52.

[18] A. Wolf, K. G. Bhushan, I. Ben-Itzhak, N. Alstein, D. Zajfman, O. Heber, and M. L. Rappaport, "Lifetime measurements of He$^-$ using an electrostatic ion trap," Phys. Rev. A **59**, 267–270 (1999).

[19] R. S. Van Dyck Jr., D. L. Farnham, and P. B. Schwinberg, "Precision mass measurements in the UW-PTMS and the electron's 'atomic mass'," Phys. Scr., T **60**, 134–143 (1995).

[20] R. M. Feenstra, "Electrostatic potential for a hyperbolic probe tip near a semiconductor," J. Vac. Sci. Technol. B **21**, 2080–2088 (2003).

[21] S. Eppell, F. R. Zypman, and R. Marchant, "Probing the resolution limits and tip interactions of AFM in the study of globular proteins," Langmuir **9**, 2281–2288 (1993).

[22] P. Lorrain, D. R. Corson, and F. Lorrain, *Electromagnetic Phenomena* (Freeman, New York, 2000), pp. 59–62.

[23] Reference 3, Sec. 3.4.

[24] G. Bennett, R. Larsen, W. Morse, Y. Semertzidis, J. Yelk, and Z. Liu, "Electrostatic quadrupole focusing in the AGS g=2 storage ring," 1993 Proceedings of the Particle Accelerators Conference, IEEE, Washington, DC, 1993, Vol. 3, pp. 2070–2072.

[25] H. S. Cohl, J. E. Tohline, A. R. P. Rau, and H. M. Srivastava, "Developments in determining the gravitational potential using toroidal functions," Astron. Nachr. **321**, 363–373 (2000).

[26] A. van Oudenaarden, M. H. Devoret, Y. V. Nazarov, and J. E. Mooij, "Magneto-electric Aharonov-Bohm effect in metal rings," Nature (London) **391**, 768–770 (1998).

ONLINE COLOR FIGURES AND AUXILIARY MATERIAL

AJP will now use author-provided color figures for its online version (figures will still be black and white in the print version). Figure captions and references to the figures in the text must be appropriate for both color and black and white versions. There is no extra cost for online color figures.

In addition AJP utilizes the Electronic Physics Auxiliary Publication Service (EPAPS) maintained by the American Institute of Physics (AIP). This low-cost electronic depository contains material supplemental to papers published through AIP. Appropriate materials include digital multimedia (such as audio, movie, computer animations, 3D figures), computer program listings, additional figures, and large tables of data.

More information on both these options can be found at www.kzoo.edu/ajp/.